

Coulomb heating of channeled H_2^+ and H_3^+ molecules in Si

R. C. Fadanelli, P. L. Grande, M. Behar, and J. F. Dias

Instituto de Física da Universidade Federal do Rio Grande do Sul, Avenida Bento Gonçalves 9500, 91501-970, Porto Alegre, Rio Grande do Sul, Brazil

G. Schiwietz

Hahn-Meitner-Institut, Abteilung, SF4 Glienicke Strasse 100, D-14109 Berlin, Germany

C. D. Denton

Departamento de Física, UTFSM, Valparaiso, Chile

(Received 17 March 2004; published 16 June 2004)

Si-*K* x-ray and backscattering yields have been measured as a function of the projectile entrance angle for atomic and molecular (H_2^+ and H_3^+) hydrogen ions channeling at kinetic energies of 150 keV per proton along the Si $\langle 100 \rangle$ crystal direction. A large enhancement of the x-ray production has been observed for well-aligned H_3^+ molecule beams. It is shown that this effect results from the Coulomb explosion of the molecule fragments during the channeling motion. Moreover, the shape and intensity of the measured angular distribution allows a quantitative determination of the corresponding heating of the transversal ion motion (2.6 ± 0.6 eV for H_2^+ and 5.1 ± 0.8 eV for H_3^+ molecules) in the channel. These values are consistent with the stored potential energies per particle and they depend significantly on the collective wake forces and molecular alignment conditions.

DOI: 10.1103/PhysRevB.69.212104

PACS number(s): 61.85.+p, 34.50.Bw, 36.40.-c, 68.55.Ln

Beams of molecules and cluster ions are useful tools in fundamental research with promising applications in material science and plasma physics. In particular, significant coherence effects (vicinage effects) have been predicted theoretically and in some cases experimental stopping forces for these structured projectiles show clear deviations from simple additive rules concerning the projectile constituents.^{1,2} Other effects related to the correlated motion of cluster atoms, such as Coulomb explosion,³ enhanced electron emission,⁴ desorption and sputtering^{5,6} have also been reported and reviewed in recent publications.⁷

In the case of crystalline materials, ions entering nearly parallel to a particular crystal axis or plane become channeled as their motion is guided by correlated collisions with target atoms. The average transversal momentum of channeled atomic particles increases due to the inelastic scattering with the target electrons and scattering at displaced target atoms. This effect enhances the number of close encounters with the atomic rows and is named transverse heating. Recently, it has been observed that charge changing processes of fast heavy ions may even lead to transversal cooling, namely, a reduction of the transversal energy.⁸

In addition to the channeling motion, molecular ions undergo a breakup process, since they lose their bonding electrons due to ionization in the first monolayers of the material. The combination of these two correlated motions, namely, the ion channeling and the breakup of the cluster under quasi-Coulombic forces, leads to a transverse Coulomb heating. Pioneering investigations of this Coulomb heating have been performed in transmission⁹ as well as using measured energy spectra of backscattered protons from H^+ , H_2^+ , and H_3^+ beams.¹⁰ However, although the effect is visible in the dechanneling profile, it was not evaluated quantitatively and has been strongly overestimated by recent computer simulations.¹¹

This paper reports on a quantitative determination of the transverse Coulomb-heating energy (abbreviated Coulomb heating) using the Si-*K* x-ray production and also the backscattering yield of molecular beams channeling along the Si $\langle 100 \rangle$ direction. Vicinage effects do not affect the *K*-shell x-ray and backscattering yields, because the characteristic impact parameters for both processes are much smaller than the typical distance for vicinage effects (2–3 Å for the present energies).² Thus, differences between experimental results for incident protons and molecular hydrogen ions are directly linked to the Coulomb explosion during the channeling motion. Finally, the experimental results for the Coulomb heating will be compared to results of advanced computer simulations.

The experiments were carried out at the Ion-Implantation Laboratory of the Federal University of Rio Grande do Sul. The 500 kV electrostatic accelerator has delivered beams of H^+ , H_2^+ , and H_3^+ at 150 keV/amu with an average current reduced down to about 35 nA for H_3^+ , 50 nA for H_2^+ , and 100 nA for H^+ . In order to ensure identical conditions, we kept the same proton flux hitting the target for all particles and clusters under study. Furthermore, the currents were reduced by an additional factor of 10 in the case of backscattering measurements. The Si $\langle 100 \rangle$ crystal was mounted on a goniometer for the alignment procedure.¹² We have fixed the azimuthal angle $\phi = 22.5^\circ$ (relative to the plane $\{1\ 0\ 0\}$) in order to avoid a full azimuthal averaging procedure around the $\langle 100 \rangle$ channel, which would be time consuming and could lead to unacceptable damage of the sample. The vacuum system of the analyzing chamber consists of an oil-free turbomolecular drag pump with a liquid nitrogen trap, capable of reaching a final pressure below 10^{-7} mbar. The samples were cleaned and etched using 10% HF before each measurement to remove the native surface oxide film.

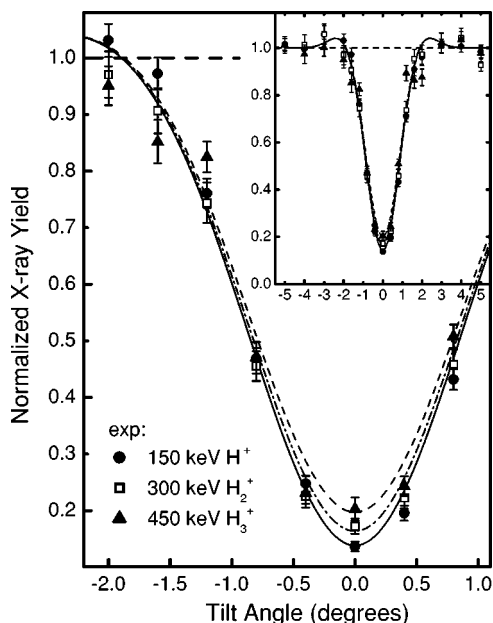


FIG. 1. Normalized x-ray yield as a function of the tilt angle for different projectiles. Increasing x-ray yields at the center of the channel are the signature of the transversal heating for H_2^+ and H_3^+ due to the Coulomb explosion. The lines are fit curves according to Eq. (1). See text for further details.

The backscattered particles were detected by a Si surface-barrier detector located at 170° with respect to the incoming beam. The overall resolution of the detection system was around 7 keV for protons. The 1.74 keV K_α x rays emitted from the target were detected by a high purity Ge detector with an energy resolution of 180 eV at 5.9 keV. This detector was mounted at 135° with respect to the beam. This constrained the measurements only to directions about the Si $\langle 100 \rangle$ one.

In order to control the damage of the Si crystal and the deposition of hydrocarbons on the surface during the angular scanning procedure, we have performed the measurements sequentially from negative tilt angles to positive ones and no differences (within the error bars) have been observed. This is a very stringent condition, since the x-ray emission is sensitive to defect creation and amorphization inside the target. Furthermore, other parameters such as target temperature, beam spot size and current density have been slightly changed and no influence has been observed on our final results.

Measurements of close encounter events giving rise to x-ray emission and backscattering under channeling conditions provide a sensitive method to investigate variations and redistribution of the ion flux close to a row of atoms, and can be used to quantify heating or cooling processes inside crystal channels. The results for the x-ray emission induced by H^+ , H_2^+ , and H_3^+ beams at 150 keV/amu are depicted in Fig. 1 as a function of the projectile entrance angle (tilt angle) for the nonplanar azimuthal angle $\phi=22.5^\circ$ relative to the plane $\{100\}$. Here, large tilt angles correspond to a nearly random direction. As can be observed from the figure, atomic and molecular beams at the same energy, flux and fluence per

atom act differently in the induced x-ray production in Si. First it is emphasized that we do not observe any molecular effects at random directions (the yields normalized to the incident proton flux are equal to within our relative errors of 4% for the difference of two spectra). Thus, we conclude that vicinage effects play no significant role for our case and correspondingly we have renormalized the spectra by about $\pm 2\%$ to exactly match each other at large angles. However, there are significant deviations at small polar angles. In comparison to H^+ , the yields are 26% larger for H_2^+ and much larger for H_3^+ (48%) at the central channel direction. This is a clear signature of the heating of the transversal motion due to Coulomb explosion. The fragment ions are pushed against the channel walls, thereby increasing the number of close encounters. In what follows we will focus on the minimal value at the axial position (and not on the shape of the channeling dip) because it is less affected by the present experimental uncertainties.

In order to estimate the value of heating or enhancement of the transversal energy, we assume that the time for the Coulomb explosion is much shorter than the typical time for a single particle to get channeled (typically the period of a channel oscillation). Under this assumption, the Coulomb explosion acts like an initial beam divergence or “astigmatic lens”¹³ and increases the initial transversal energy by an effective Coulomb-heating energy δE_C . Since the initial transversal energy E_T depends on the incident entrance angle [through the relation $E_T = E\Psi^2 + U(\vec{r})$, where E is the ion energy and U is the channeling potential], the additional Coulomb energy component δE_C will be equivalent to a tilt offset ($\Psi \rightarrow \sqrt{\Psi^2 + \delta E_C/E}$). Thus, the yield for the molecular channeling will be modified in comparison to the atomic one by

$$Y_{\text{molecular}}(\Psi) = Y_{\text{atomic}}(\sqrt{\Psi^2 + \delta E_C/E}). \quad (1)$$

This scaling behavior can also be derived considering the angular distribution due to the Coulomb explosion and a parabolic dependence for the yield. Using the equation above and an analytic expression for Y_{atomic} which fits the H dip curve very well (solid curve), we obtain the broken curves in Fig. 1 that fit the experimental data best for molecular beams. In this way, the transverse Coulomb heating energies evaluated for H_2^+ and H_3^+ are $\delta E_C = 1.8 \pm 1.0$ eV and 4.8 ± 2.0 eV, respectively.

The transverse Coulomb energy is regarded to be an averaged value and is about the stored internal energy per particle \mathcal{U} inside the solid (namely, $2\mathcal{U}/3$ in the case of spherical averaging). The above heating energies are consistent with \mathcal{U} evaluated from the Yukawa potential with the screening length given by the ion velocity v and plasmon energy ω_p ($\lambda = v/\omega_p$). However, the free-Coulomb energies of 5.8 eV for H_2^+ and 14.4 eV per proton for H_3^+ molecules are completely inconsistent with the experimental results.

Despite its simplicity, providing values for the transverse heating energies in a straightforward manner, it must be stressed that the above estimate does not take into account the fact that the Coulomb explosion is indeed not instantaneous, and therefore acts as a beam divergence only after the

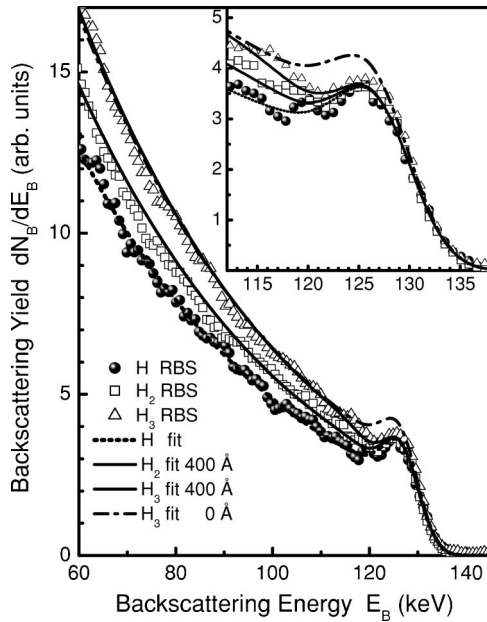


FIG. 2. RBS yield as a function of the energy. Curves stand for the fitting procedure according to the two-beam model assuming that the Coulomb explosion effectively takes place at the surface (0 Å: dashed-dotted curve for H_3^+) and at a critical depth of 400 Å (solid lines).

ions penetrate a given distance in the solid. This effect can be observed in the backscattering data since the measured final proton energy contains information on the depth scale of the backscattering/dechanneling events.

Figure 2 shows Rutherford backscattering spectra (RBS) for well channeled ($\Psi=0$) H^+ , H_2^+ , and H_3^+ incident ions at 150 keV/amu normalized to the spectra taken at a random incidence. As can be observed from this figure, the backscattering yield just below the surface peak is nearly the same for atomic and molecular ions, whereas for detected energies below 110 keV (deep inside the solid) the yields and slopes are indeed different. This shows that the effect of the Coulomb explosion enhances the dechanneling only after a certain penetration depth. The data have been fitted (see solid and dashed lines) using the two-beam model.¹⁴ The dechanneled beam fraction χ is given by

$$\frac{d\chi}{dx} = \alpha[1 - \chi(x)], \quad (2)$$

where α is the dechanneling rate and $1 - \chi(x)$ is the channeled fraction of the beam. The dechanneling rate α was chosen to be independent on the penetrated distance x for H^+ ions and its value has been determined for each incident angle Ψ . The dashed curve for H_3^+ was obtained by fixing all parameters as for H^+ projectiles except for the α parameter that was changed according to the ansatz from Eq. (1), namely, $\alpha_{\text{molecular}} = \alpha_{\text{atomic}}(\Psi = \sqrt{\delta E_C/E})$. Moreover, the best fitting (solid lines) is obtained by introducing a depth Δx_C below which the α parameter is taken to be the same as for H^+ ions for $\Psi=0$. For this analysis we have used the electronic stopping to convert the energy loss in depth x as well

TABLE I. Experimental Coulomb-heating energies (in eV) obtained in this work for two critical depths Δx_C using Eq. (1) and also the two-beam model (TBM). The last row contains the most accurate results (see text).

Δx_C	x ray [Eq. (1)]		RBS (TBM)		x ray (TBM)	
	H_2	H_3	H_2	H_3	H_2	H_3
0 Å	1.8 ± 1.0	4.8 ± 2.0	2.9 ± 0.7	4.4 ± 1.0	1.5 ± 1.0	4.7 ± 2.0
400 Å			3.0 ± 1.0	5.0 ± 1.0	2.0 ± 1.2	5.9 ± 2.0

the Rutherford cross section to determine the backscattering yield.¹⁵ In addition, the spectrum has been convoluted with the experimental resolution and energy loss straggling.

The RBS results for the Coulomb heating are displayed in Table I for $\Delta x_C=0$ and $\Delta x_C=400$ Å (the best fit). The x-ray data have also been evaluated more rigorously using the above discussed two-beam model by integrating the x-ray yield arising from different depths. The main difference with RBS simulations is the use of the x-ray production cross section.¹⁶

The improved x-ray results, also included in Table I, are in very good agreement with those from the RBS analysis. It is pointed out that the results presented in Table I do not change significantly for different choices of Δx_C . In addition, the distance of 400 Å is also consistent with the simulation using full wake forces to describe the breakup process. We note that the simple assumption of a screened Coulomb potential such as the Yukawa potential would lead to much shorter breakup distances.

These results have been compared to full calculations of the molecular breakup under the influence of quasi-Coulombic forces, channeling, and electronic energy loss (elastic and inelastic scattering processes) as the calculations from Ref. 17. Briefly, the breakup force, which is present only in the case of molecular projectiles, is the screened Coulomb repulsion between the fragments. The screening is modeled by a wake-type potential obtained by the linear dielectric formalism. The description of the dielectric properties of the target (silicon) is based on a Mermin dielectric function.¹⁸ In addition, the channeling force is the repulsive interaction with the crystal nuclei and it is modeled using a Molière potential and thermal vibrations with a 1D r.m.s. amplitude of $\sigma=0.08$ Å.¹⁹ Fluctuations in the energy loss and inelastic multiple scattering of the projectile are also included in the calculations. We have considered the possibility that about 10% of the protons may be neutralized in Si, which reduces the Coulomb explosion. However, this small presence of H^0 would affect the Coulomb heating only by less than 5%. Using this program we are able to obtain fundamental quantities such as the flux distribution of particles within the channel as well as the distribution of transversal energies as a function of the penetration depth.

Theoretical values for the distribution of transversal energies are plotted in Fig. 3 for protons, H_2^+ and H_3^+ molecules after penetrating a distance of 4000 Å (for larger distances the Si- K ionization cross section is negligible). In the case of protons, the plot corresponds essentially to the initial transversal energy distribution since inelastic multiple scattering

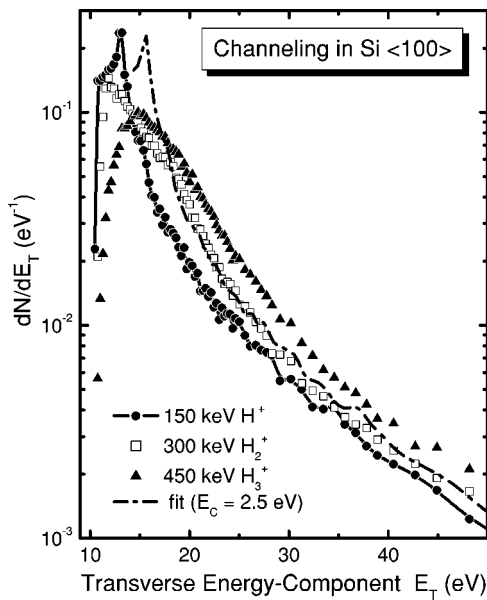


FIG. 3. Simulated transversal-energy distribution for H^+ , H_2^+ , and H_3^+ ions. The dashed-dotted curve shows the H^+ data shifted by a heating energy of 2.5 eV in order to match the H_2^+ distribution at energies above 20 eV.

is of minor importance. As observed in Fig. 3, the transversal energy distributions for the molecular ions are shifted to higher energies, a consequence of the Coulomb-heating process. The theoretical values of the Coulomb heating (2.5 ± 0.2 for H_2^+ and 4.5 ± 0.2 for H_3^+) were obtained by shifting the atomic distribution (solid curve) to agree with the molecular one at higher transversal energies (dashed-dotted curve), since close encounter events are mainly due to these energies.

The theoretical values for δE_C agree with the experimental ones to within our error bars. These values are much

smaller than the stored free-Coulomb energy because of the solid-state screening and alignment conditions due to the wake and channeling forces. Fragments such as H_2^+ tend to align themselves because the wake forces have a larger longitudinal (along the velocity direction) component. Once the molecule is aligned, the explosion is fully longitudinal, and the heating effect disappears. This alignment condition may also explain the conflicting interpretation in Ref. 11. The simulations in this reference have strongly overestimated the experimental data for H_2^+ projectiles, because no wake forces have been included in these calculations.

In summary, we have investigated the proton backscattering yield and Si-K x-ray production due to channeling of molecular ions along the Si $\langle 100 \rangle$ direction as a function of the projectile entrance angle. Measurements using atomic and molecular H_2^+ and H_3^+ beams at kinetic energies of 150 keV per proton have been used to test a method for obtaining direct information about the interplay of molecular Coulomb explosion, screening, and wake forces inside of solid. We have shown that the present method of analyzing angle-dependent x-ray and backscattering data is an excellent tool for determining the ion-flux redistribution related to the Coulomb explosion against the channel walls.

A heating of the transversal fragment-ion motion is observed in the x-ray yield and also evaluated quantitatively for both types of measurements. Our method provides consistent values for the Coulomb-heating energy in a straightforward manner. Furthermore, the experimental values are in good agreement with theoretical results. In future applications, the Coulomb heating might be used to tailor high-energy channeling-implantation profiles of heavy molecular ions by a proper choice of the number of cluster constituents.

This work was partially supported by the Brazilian agencies CNPq, CAPES and by the cooperation programs PROBRAL 166/04 and SETCIP/CAPES 33/01.

¹W. Brandt, A. Ratkowski and R. H. Ritchie, Phys. Rev. Lett. **33**, 1325 (1974).

²N. R. Arista, Nucl. Instrum. Methods Phys. Res. B **164-165**, 108 (2000).

³D. S. Gemmell *et al.*, Phys. Rev. Lett. **34**, 1420 (1975).

⁴H. Rothard *et al.*, Phys. Rev. B **41**, 3959 (1990).

⁵T. Yamaguchi *et al.*, Nucl. Instrum. Methods Phys. Res. B **99**, 237 (1995).

⁶N. Toyoda, J. Matsuo, and I. Yamada, *Proceedings of the 14th International Conference on Application of Accelerators in Research and Industry*, AIP Conf. Proc. No. 392 (AIP Press, New York, 1997), p. 483.

⁷I. Yamada, J. Matsuo, and N. Toyoda, Nucl. Instrum. Methods Phys. Res. B **206**, 820 (2003).

⁸W. Assmann *et al.*, Phys. Rev. Lett. **83**, 1759 (1999).

⁹J. C. Poizat and J. Remillieux, J. Phys. B **5**, L94 (1972).

¹⁰J. M. Caywood, T. A. Tombrello, and T. A. Weaver, Phys. Lett.

37A, 350 (1971); T. A. Tombrello and J. M. Caywood, Phys. Rev. B **8**, 3065 (1973).

¹¹V. A. Khodyrev, V. S. Kulikauskas, and C. Yang, Nucl. Instrum. Methods Phys. Res. B **195**, 259 (2002).

¹²G. de M. Azevedo *et al.*, Phys. Rev. B **65**, 075203 (2002).

¹³P. Sigmund, Nucl. Instrum. Methods Phys. Res. B **67**, 11 (1992).

¹⁴G. Götz and K. Gärtner, *High Energy Ion Beam Analysis of Solids* (Akademie-Verlag, Berlin, 1988).

¹⁵W. K. Chu, J. W. Mayer, M.-A. Nicolet, *Backscattering Spectrometry* (Academic Press, New York, 1978).

¹⁶J. L. Campbell and J. A. Maxwell, *Compilation of the atomic physics database for the GUPIX program*.

¹⁷S. Heredia-Avalos *et al.*, Phys. Rev. Lett. **88**, 079601 (2002).

¹⁸I. Abril *et al.*, Phys. Rev. A **58**, 357 (1998).

¹⁹W. Eckstein, *Computer Simulation of Ion-Solid Interaction* (Springer-Verlag, Berlin, 1991).